


# Commercialization of Micro-fabrication of Antenna-Coupled Transition Edge Sensor Bolometer Detectors for Studies of the Cosmic Microwave Background

Aritoki Suzuki<sup>1</sup>  · Chris Bebek<sup>1</sup> · Maurice Garcia-Sciveres<sup>1</sup> · Stephen Holland<sup>1</sup> · Akito Kusaka<sup>1,5</sup> · Adrian T. Lee<sup>1,2,3</sup> · Nicholas Palaio<sup>4</sup> · Natalie Roe<sup>1</sup> · Leo Steinmetz<sup>2</sup>

Received: 4 November 2017 / Accepted: 29 March 2018 / Published online: 9 April 2018  
© Springer Science+Business Media, LLC, part of Springer Nature 2018

**Abstract** We report on the development of commercially fabricated multichroic antenna-coupled transition edge sensor (TES) bolometer arrays for cosmic microwave background (CMB) polarimetry experiments. CMB polarimetry experiments have deployed instruments in stages. Stage II experiments deployed with O(1000) detectors and reported successful detection of B-mode (divergence-free) polarization pattern in the CMB. Stage III experiments have recently started observing with O(10,000) detectors with wider frequency coverage. A concept for a stage IV experiment, CMB-S4, is emerging to make a definitive measurement of CMB polarization from the ground with O(400,000) detectors. The orders of magnitude increase in detector count for CMB-S4 require a new approach in detector fabrication to increase fabrication throughput and reduce the cost. We report on collaborative efforts with two commercial micro-fabrication foundries to fabricate antenna-coupled TES bolometer detectors. The detector design is based on the sinuous antenna-coupled dichroic detector from the POLARBEAR-2 experiment. The TES bolometers showed the expected I–V response, and the RF performance agrees with the simulation. We will discuss the motivation, design consideration, fabrication processes, test results, and how industrial detector fabrication could be a path to fabricate hundreds of detector wafers for future CMB polarimetry experiments.

---

✉ Aritoki Suzuki  
asuzuki@lbl.gov

<sup>1</sup> Physics Division, Lawrence Berkeley National Laboratory, Berkeley, CA 94720, USA

<sup>2</sup> Department of Physics, University of California, Berkeley, CA 94720, USA

<sup>3</sup> Radio Astronomy Laboratory, University of California, Berkeley, CA 94720, USA

<sup>4</sup> Engineering Division, Lawrence Berkeley National Laboratory, Berkeley, CA 94720, USA

<sup>5</sup> Department of Physics, University of Tokyo, Tokyo 113-0033, Japan

**Keywords** Cosmic microwave background · TES bolometer · Micro-fabrication · Inflation · Polarization · B-mode

## 1 Introduction

Over the past 2 decades, teams from around the world have taken increasingly sensitive measurements of the cosmic microwave background (CMB) using telescopes on the ground, balloons and satellites. Its uniformity confirmed the hot big bang model of the universe, and detailed measurements of its small  $10^{-5}$  non-uniformity have led to tight constraints on the composition, geometry, and evolution of the universe. The CMB is also weakly polarized through Thomson scattering by free electrons, and it provides access to information that is inaccessible from temperature anisotropy [1].

CMB polarization can be decomposed into two orthogonal bases that are determined by the physical origins. Scalar perturbations that are also responsible for temperature anisotropy and structure formation produced the parity-conserving polarization pattern (E-mode). The existence of light particles such as neutrinos and postulated light relics, including axions and sterile neutrinos, alters the total energy density of the radiation in the radiation-dominated era of the universe to distort the E-mode power spectrum at arc-minute angular scales. At very large angular scales, the E-mode is a probe to the physics of reionization that would allow CMB measurement to tighten constraint on the sum of neutrino masses. Starting in late 2013, ground-based CMB experiments reported the detection of the parity-violating polarization pattern in the CMB, called the B-mode. Large-scale structures between the surface of last scattering and the observer deflect the E-mode polarization pattern to convert E-mode into B-mode through weak gravitational lensing. This *lensing* B-mode peaks at an arc-minute angular scale, and amplitude of its angular power spectrum constrains the sum of neutrino masses. At degree angular scale amplitude of B-mode spectrum will allow us to explore to models of inflation, a postulated time period of rapid expansion of the universe at early universe, if its energy scale was at detectable level. To explore these sciences and beyond, the field deployed CMB polarimetry experiments in stages. Stage II experiments deployed with O(1000) detectors that reported successful detection of B-mode (divergence-free) polarization pattern in the CMB. Stage III experiments have recently started observing with O(10,000) detectors with wider frequency range coverage to characterize galactic foregrounds. A concept for a stage IV experiment, CMB-S4, is emerging to make a definitive measurement of CMB polarization from the ground with O(400,000) detectors.

Concepts of configurations for the next-generation CMB experiment have been studied by the CMB communities [2, 3]. Studies found that O(400,000) detector spread across 20–300 GHz on a few large-aperture (6 m) telescopes and over a dozen small-aperture ( $\approx 0.5$  m) telescopes deployed at Chile and South Pole sites, two sites that have current CMB ground-based telescopes, which is a configuration that can achieve the science target of the next-generation CMB experiment. Concept definition task force reported that this next-generation CMB experimental configuration will achieve  $\sigma(r) \leq 0.0005$ ,  $\sigma(\Delta N_{\text{eff}}) < 0.03$ , and  $\sigma(\Sigma(m_\nu)) < 25$  meV with 5–7 years of observations.

To deploy  $O(400,000)$  detectors, the stage IV experiment will require approximately 300 150-mm yielded detector wafers. The actual number of wafers that will need to be fabricated will depend on production yield. Up until now, CMB detector wafers were micro-fabricated in clean rooms at the national laboratories and the universities by specialized engineers, technicians, postdocs, or graduate students. The orders of magnitude increase in wafer count for the stage IV experiment requires a new approach in detector fabrication to increase throughput. As a potential new approach to fabricate CMB detectors, we worked collaboratively with two commercial micro-fabrication foundries to fabricate antenna-coupled TES bolometer detectors. Industrial fabrication facilities have a potential to increase the throughput and reduce the cost per wafer by having more streamlined processes and multiple shifts. Also, stringent industrial approach on quality assurance could improve uniformity, repeatability, and yield that are necessary for the next-generation CMB experiment. We designed, fabricated, and tested prototype detectors with commercial foundries to demonstrate this new approach.

## 2 Design and Fabrication

Micro-fabrication of science grade detectors by a commercial foundry was successfully implemented by the Dark Energy Spectroscopic Survey experiment where Lawrence Berkeley National Laboratory and Teldyne DALSA Inc. co-fabricated CCDs [4]. Modern micro-fabricated CMB detectors require superconducting niobium. We collaborated with two commercial foundries that specialize in micro-fabrication of niobium devices. Two foundries, HYPRES Inc. and STAR Cryoelectronics, specialize in fabrication of superconducting devices such as Superconducting QUantum Interference Devices (SQUIDs) and voltage standards with Josephson junctions [5,6]. Both foundries were familiar with films that are commonly used in the CMB detector fabrication, such as niobium, silicon dioxide, aluminum, titanium, palladium, and silicon nitride. The detector design was based on the sinuous antenna-coupled dichroic (90 and 150 GHz) detector from the POLARBEAR-2a experiment [7]. Test chips of 20 mm by 20 mm were fabricated at STAR Cryoelectronics, and HYPRES Inc. co-fabricated 271 pixel detector arrays, as shown in Fig. 1.

Detectors were fabricated on 150-mm-diameter silicon wafers at both foundries. Fabrication steps were based on the POLARBEAR-2 detector design that was developed at the Marvell Nanofabrication Laboratory of the University of California, Berkeley [8]. STAR Cryoelectronics processed every step of fabrication at their facility. STAR Cryoelectronics devices were fabricated with aluminum transition edge sensors (TESs). HYPRES co-fabricated wafers with the UC Berkeley Nanofabrication Laboratory. Most processes were completed at HYPRES, and then deposition of aluminum–manganese film and bolometer release step with xenon difluoride gas were done at the UC Berkeley Nanofabrication Laboratory. Fabrication of each layer requires deposition, lithography, etching, cleaning, and characterization. Both fabrication foundries spent a day per layer with a single shift per day. We can further increase production rate by increasing the number of shifts per day to meet future demands. Absolute film thickness and its uniformity across wafers were measured with ellip-

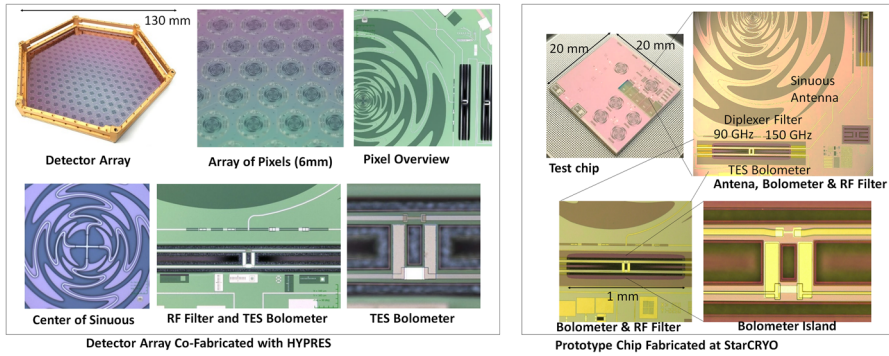


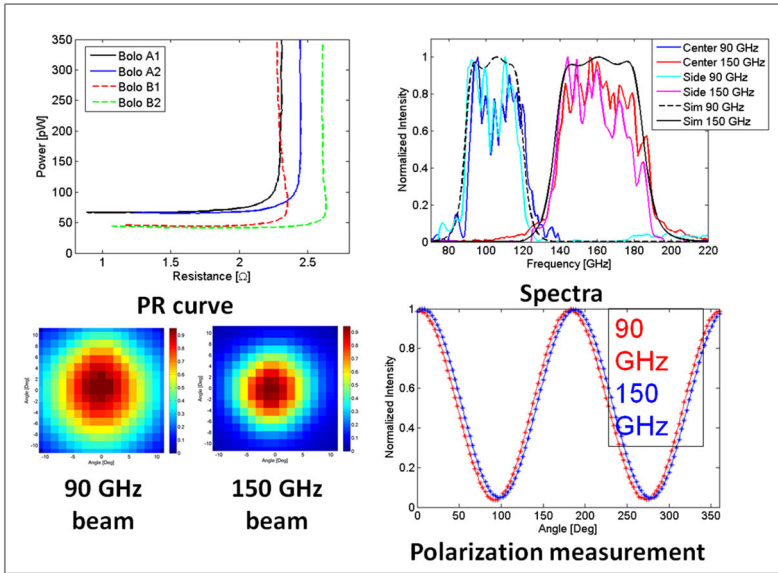
**Fig. 1** [Left] Photographs of sinuous antenna-coupled detector array fabricated with HYPRES. Top row from left: hexagonal detector array mounted in POLARBEAR-2 detector holder, zoomed in array of pixels that are 6.8 mm apart, and overview of a pixel with sinuous antenna and TES bolometer highlighted. Bottom row from left: zoomed in photograph at center of sinuous antenna showing 2-micron-wide feed, RF diplexer filter and TES bolometer, and zoomed in at center of bolometer island. Bright white rectangle in the zoomed in photograph of the bolometer island is an AlMn TES bolometer. [Right] Photograph of sinuous antenna-coupled detector test chip fabricated by STAR Cryoelectronics. Several test devices were fabricated on 20 mm by 20 mm chips. Zoomed in photographs show pixel overview, including the sinuous antenna, RF filter, and TES bolometer (Color online)

someter and profilometer during fabrication processes. The silicon oxide film has the tightest tolerance, as its variation in thickness across a wafer will result in shifts of the center frequency of the detectors band-pass filter. Film thickness variation of this film was less than 2% which meets the current experiment’s specification. STAR Cryoelectronics yielded detectors on three of three fabricated wafers. HYPRES delivered four of five wafers with high detector yield, with one of the original five wafers sacrificed for fabrication process development.

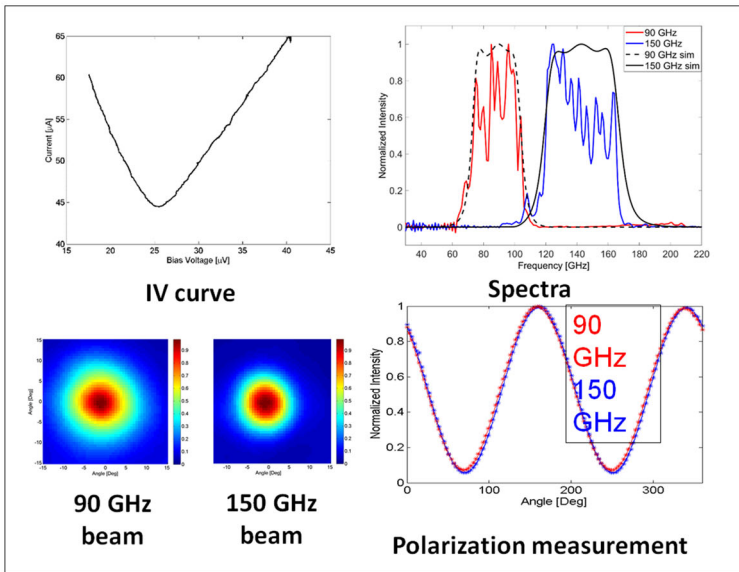
### 3 Test Results

Delivered wafers were characterized at room temperature first for DC connectivity. We developed a computer program for the motor-actuated automatic micro-probe station to probe through approximately 1600 detectors on a detector array wafer. We checked for thru, shorts to neighboring channel, and undesirable shorts to ground layer. This automated probe station can scan through 1600 detectors in about an hour. We defined electrical yield as the number of detectors that show nominal resistance, are not shorted to neighbor, and do not show short to ground. Highest electrical yield was 97%. All wafers had yield above 90%. Most yield losses were due to broken niobium traces between TES bolometers and wire bond pads.

A brief description of the test setups are given below. A detailed description can be found elsewhere [9]. Characterization of detectors at cryogenic temperature was conducted in an eight-inch Infrared Labs wet dewar with helium-3 adsorption fridge that achieves a 250 milli-Kelvin base temperature. The dewar is equipped with Quantum Design DC SQUID readout electronics. Voltage biases to TES bolometers were provided by a battery at room temperature connected to a 20 milli-Ohm shunt resis-



**Test results from devices from HYPRES**



**Test results from devices from STAR Cryoelectronics**

**Fig. 2** Performance of fabricated devices from HYPRES (top) and STAR Cryoelectronics (bottom). Upper left figure shows electrical bias power versus resistance curve for TES bolometers for two different frequency bands from two different locations on a wafer from HYPRES wafer. Current versus bias voltage plot is shown for STAR Cryoelectronics device. Upper right panel shows spectra measurement by Fourier transform spectrometer. Bottom left plot shows angular response of a multichroic detector to a temperature-modulated source. Bottom right figure shows polarization response of a detector to a rotating wire grid in front of a temperature-modulated source (Color online)

tor mounted on the 4 Kelvin stage. For TES bolometer characterization, we enclosed detectors in a 250 milli-Kelvin metal enclosure to block out stray optical power. For optical tests, we mounted the detector chip on an anti-reflection-coated synthesized elliptical alumina lens. The dewar has a zotefoam optical window with metal mesh low-pass filters provided by Cardiff University. A Michelson Fourier transform spectrometer with a 254-micron-thick Mylar beam splitter was used to characterize the spectral response. Angular responses were characterized by scanning a 12.7-mm-diameter temperature-modulated source in front of a dewar window on a 2-D linear actuated stage. Polarization responses were characterized by rotating a wire grid in front of the temperature-modulated source located at the peak of the antenna angular response.

Plots of detector performances are shown in Fig. 2. Devices from both foundries showed the expected current-to-voltage responses with two distinct regions of constant resistance and constant power. Devices from STAR Cryoelectronics were fabricated with aluminum TES that has a superconducting transition temperature of approximately 1.2 Kelvin to fabricate bolometers with saturation power around 1000 pW for laboratory optical performance characterization using bright source. Wafers from HYPRES were fabricated with an aluminum–manganese film. TES bolometers that have different weak link leg lengths (830 vs 630 micron) had saturation powers of 45 and 67 pW, respectively. This nearly follows the inverse leg length relationship. The absolute value of the saturation power was higher than desirable because the critical temperature of TESs were higher than what we targeted. We targeted a TES critical temperature of 450 milli-Kelvin, but the tested chip had a critical temperature of 650 milli-Kelvin. This discrepancy was expected. The critical temperature of the aluminum–manganese film is reported to depend on the temperature that a film is heated to during the fabrication process, the underlying layer's composition and sputter condition [10]. Our goal was to demonstrate a working TES bolometer; we did not fine-tune the heating temperature of a wafer for this round of fabrication. It is our goal for future fabrications to fine-tune heating temperature to optimize aluminum–manganese's critical temperature. For detector array from HYPRES, we also compared uniformity across the wafer. TES bolometers were randomly selected from the center and very edge of detector wafer for characterization. We saw  $\pm 2\%$  variation in saturation power between two pixels; this is well within our tolerance. TES bolometers for two chips showed  $\pm 5\%$  variation in bolometer resistance. This is mostly due to the wet etching process that was used to define aluminum–manganese, which is inherently difficult to control dimension to a high tolerance. For future fabrication, we decided to adapt ion milling to define aluminum–manganese TES for higher tolerance.

Spectra measurements show that the RF filter worked as expected, as the signal from the broadband sinuous antenna is split into 90 and 150 GHz frequency bands and matches well with simulation. These filters were designed without prior measurement of material properties from the foundries. Measurement of reasonable band location and shape suggests that the material properties of films from these foundries are close to what we obtain from academic foundries. For HYPRES wafers, we also looked at the spread in band-pass frequency by comparing randomly chosen pixels from the center and edge of a detector array. Band-pass center frequency shifts between center pixel and edge pixel were downward shifted by 2 GHz for 90 GHz band and 1 GHz

for 150 GHz band. Bandwidths were consistent between these pixels, and band-pass shapes are similar as shown in Fig. 2.

Beam measurements show a round beam with devices from both foundries. Ellipticity, defined as the difference in beam width divided by the sum of beam width, was  $2 \pm 1$  and  $1 \pm 1\%$  for 90 and 150 GHz, respectively, for devices from STAR Cryoelectronics and  $3 \pm 1$  and  $2 \pm 1\%$  for 90 and 150 GHz, respectively, for devices from HYPRES. We also looked at uniformity for HYPRES detector arrays. The spread in 150 GHz beam size was  $4.9^\circ \pm 0.2^\circ$  and  $5.1^\circ \pm 0.1^\circ$  for center and edge pixels, respectively. Beam ellipticity of 150 GHz was  $3 \pm 1$  and  $1 \pm 1$  for center and edge pixels, respectively.

Polarization response was characterized by a rotating wire grid between the dewar and the temperature-modulated source. Polarization leakage measurement results were setup dependent. Results were sensitive to how the grid was tilted and shielded with respect to the dewar window. We report measured value as an upper limit as an improved setup may show lower leakage. For devices from STAR Cryoelectronics, we measured polarization leakage upper limits of 7 and 6% for 90 and 150 GHz, respectively. For devices from HYPRES, we measured upper limits of 4 and 5%, respectively.

## 4 Conclusion and Future Developments

We successfully designed, fabricated, and tested antenna-coupled TES bolometer devices with commercial foundries. Transfer of fabrication processes was done successfully between scientists at the national laboratory and engineers at the foundries. Production rate was high, and wafers were delivered with high yield. Fabricated TES bolometers were successfully biased and readout by SQUID readout electronics. Fabricated RF structures were sensitive to millimeter wave signals with their performance mostly matching with the simulations. To push further on this approach, our next goal is to make an antenna-coupled bolometer detector array with optimized characteristics that is suitable for CMB observation. We would also like to demonstrate repeatability and production rate of the foundry to prepare for the next-generation CMB experiment. R&D on fabricating superconducting devices at commercial foundries not only benefits future CMB experiment, but also provides more fabrication options for other fields that need superconducting devices such as the Quantum Information Science and Dark Matter experiment.

**Acknowledgements** This work was supported by Laboratory Directed Research and Development (LDRD) funding from Berkeley Lab, provided by the Director, Office of Science, of the US Department of Energy under Contract No. DE-AC02-05CH11231. We thank Dr. Daniel Yohannes, Dr. Oleg Mukhanov, and Dr. Alex Kirichenko from HYPRES Inc. for valuable suggestions and feedback that led to successful fabrication. We thank Dr. Robin Cantor from STAR Cryoelectronics for valuable suggestions and feedback that led to successful fabrication.

## References

1. N. Kevork, Abazajian et al., CMB-S4 Science Book, 1st edn (2016). [arXiv:1610.02743](https://arxiv.org/abs/1610.02743)

2. Concept Definition Task Force (2017) Cosmic microwave background stage 4 concept definition task force. [https://cmb-s4.org/CMB-S4workshops/images/CMBS4\\_CDT\\_final.pdf](https://cmb-s4.org/CMB-S4workshops/images/CMBS4_CDT_final.pdf). Accessed 4 Nov 2017
3. D. Barron, Y. Chinone, A. Kusaka, J. Borril, J. Errard, S. Feeney, S. Ferraro, R. Keskitalo, A.T. Lee, N.A. Roe, B.D. Sherwin, A. Suzuki, Optimization study for the experimental configuration of CMB-S4, JCAP (2017). [arXiv:1702.07467](https://arxiv.org/abs/1702.07467)
4. C.J. Bebek, J.H. Emes, D.E. Groom, S. Haque, S.E. Holland, P.N. Jelinsky, A. Karcher, W.F. Kolbe, J.S. Lee, N.P. Palaio, D.J. Schlegel, G. Wang, R. Groulx, R. Frost, J. Estrada, M. Bonati, Status of the ccd development for the dark energy spectroscopic instrument. J. Instrum. **12**(04), C04018 (2017)
5. HYPRES Inc. (2017) HYPRES Inc. <http://www.hypres.com/>. Accessed 4 Nov 2017
6. STAR Cryoelectronics (2017) STAR Cryoelectronics. <https://starcryo.com/>. Accessed 4 Nov 2017
7. A. Suzuki, K. Arnold, J. Edwards, G. Engargiola, W. Holzappel, B. Keating, A.T. Lee, X.F. Meng, M.J. Myers, R. OBrient, E. Quealy, G. Rebeiz, P.L. Richards, D. Rosen, P. Siritanasak, Multi-chroic dual-polarization bolometric detectors for studies of the cosmic microwave background. J. Low Temp. Phys. **176**(5–6), 650–656 (2014)
8. B. Westbrook et al., The polarbear-2 and simons array focal plane fabrication status. J. Low Temp. Phys. (under review)
9. A. Suzuki, Multichroic bolometric detector architecture for cosmic microwave background polarimetry experiments. Ph.D. thesis, University of California, Berkeley (2013)
10. D. Li, J.E. Austermann, J.A. Beall, D.T. Becker, S.M. Duff, P.A. Gallardo, S.W. Henderson, G.C. Hilton, S.-P. Ho, J. Hubmayr, B.J. Koopman, J.J. McMahon, F. Nati, M.D. Niemack, C.G. Pappas, M. Salatino, B.L. Schmitt, S.M. Simon, S.T. Staggs, J. Van Lanen, J.T. Ward, E.J. Wollack, Almn transition edge sensors for advanced actpol. J. Low Temp. Phys. **184**(1), 66–73 (2016)